Evidence for the $\eta_b(2S)$ and Observation of $h_b(1P) \to \eta_b(1S)\gamma$ and $h_b(2P) \to \eta_b(1S)\gamma$

R. Mizuk,[16] D. M. Asner,[40] A. Bondar,[1] T. K. Pedlar,[25] I. Adachi,[9] H. Aihara,[50] K. Arinstein,[1] V. Aulchenko,[1] T. Aushev,[16] T. Aziz,[46] A. M. Bakich,[45] A. Bay,[23] K. Belous,[14] V. Bhardwaj,[31] B. Bhuyan,[10] M. Bischofberger,[31] G. Bonvicini,[55] A. Bozek,[35] M. Bračko,[26,17] J. Brodzicka,[35] T. E. Browder,[8] V. Chekelian,[27] A. Chen,[32] P. Chen,[34] B. G. Cheon,[7] K. Chilikin,[16] R. Chistov,[16] I.-S. Cho,[57] K. Cho,[20] S.-K. Choi,[6] Y. Choi,[44] J. Dalseno,[27,47] M. Danilov,[16] Z. Doležal,[2] Z. Drásal,[2] A. Drutskoy,[16] S. Eidelman,[1] D. Epifanov,[1] J. E. Fast,[40] V. Gaur,[46] N. Gabyshev,[1] A. Garmash,[1] B. Golob,[24,17] J. Haba,[9] T. Hara,[9] K. Hayasaka,[30] H. Hayashii,[31] Y. Horii,[30] Y. Hoshi,[48] W.-S. Hou,[34] Y. B. Hsiung,[34] H. J. Hyun,[22] T. Iijima,[30,29] A. Ishikawa,[49] R. Itoh,[9] M. Iwabuchi,[57] Y. Iwasaki,[9] T. Iwashita,[31] I. Jaegle,[8] T. Julius,[28] J. H. Kang,[57] P. Kapusta,[35] T. Kawasaki,[37] H. J. Kim,[22] H. O. Kim,[22] J. H. Kim,[20] K. T. Kim,[21] M. J. Kim,[22] Y. J. Kim,[20] K. Kinoshita,[3] B. R. Ko,[21] S. Koblitz,[27] P. Kodyš,[2] S. Korpar,[26,17] R. T. Kouzes,[40] P. Križan,[24,17] P. Krokovny,[1] T. Kuhr,[19] T. Kumita,[52] A. Kuzmin,[1] Y.-J. Kwon,[57] J. S. Lange,[4] S.-H. Lee,[21] J. Li,[43] J. Libby,[11] C. Liu,[42] Y. Liu,[3] Z. Q. Liu,[12] D. Liventsev,[16] R. Louvot,[23] D. Matvienko,[1] S. McOnie,[45] K. Miyabayashi,[31] H. Miyata,[37] G. B. Mohanty,[46] D. Mohapatra,[40] A. Moll,[27,47] N. Muramatsu,[41] R. Mussa,[15] M. Nakao,[9] Z. Natkaniec,[35] C. Ng,[50] S. Nishida,[9] K. Nishimura,[8] O. Nitoh,[53] T. Nozaki,[9] T. Ohshima,[29] S. Okuno,[18] S. L. Olsen,[43] Y. Onuki,[50] P. Pakhlov,[16] G. Pakhlova,[16] C. W. Park,[44] H. Park,[22] R. Pestotnik,[17] M. Petrič,[17] L. E. Piilonen,[54] A. Poluektov,[1] M. Röhrken,[19] Y. Sakai,[9] S. Sandilya,[46] D. Santel,[3] T. Sanuki,[49] Y. Sato,[49] O. Schneider,[23] C. Schwanda,[13] K. Senyo,[56] O. Seon,[29] M. E. Sevior,[28] M. Shapkin,[14] C. P. Shen,[29] T.-A. Shibata,[51] J.-G. Shiu,[34] B. Shwartz,[1] A. Sibidanov,[45] F. Simon,[27,47] P. Smerkol,[17] Y.-S. Sohn,[57] A. Sokolov,[14] E. Solovieva,[16] S. Stanič,[38] M. Starič,[17] M. Sumihama,[5] T. Sumiyoshi,[52] K. Tanida,[43] G. Tatishvili,[40] Y. Teramoto,[39] I. Tikhomirov,[16] K. Trabelsi,[9] T. Tsuboyama,[9] M. Uchida,[51] S. Uehara,[9] T. Uglov,[16] Y. Unno,[7] S. Uno,[9] P. Vanhoefer,[27] G. Varner,[8] K. E. Varvell,[45] A. Vinokurova,[1] V. Vorobyev,[1] C. H. Wang,[33] M.-Z. Wang,[34] P. Wang,[12] X. L. Wang,[12] M. Watanabe,[37] Y. Watanabe,[18] K. M. Williams,[54] E. Won,[21] B. D. Yabsley,[45] J. Yamaoka,[8] Y. Yamashita,[36] C. Z. Yuan,[12] Z. P. Zhang,[42] and V. Zhilich[1]

(Belle Collaboration)

[1]*Budker Institute of Nuclear Physics SB RAS and Novosibirsk State University, Novosibirsk 630090*
[2]*Faculty of Mathematics and Physics, Charles University, Prague*
[3]*University of Cincinnati, Cincinnati, Ohio 45221*
[4]*Justus-Liebig-Universität Gießen, Gießen*
[5]*Gifu University, Gifu*
[6]*Gyeongsang National University, Chinju*
[7]*Hanyang University, Seoul*
[8]*University of Hawaii, Honolulu, Hawaii 96822*
[9]*High Energy Accelerator Research Organization (KEK), Tsukuba*
[10]*Indian Institute of Technology Guwahati, Guwahati*
[11]*Indian Institute of Technology Madras, Madras*
[12]*Institute of High Energy Physics, Chinese Academy of Sciences, Beijing*
[13]*Institute of High Energy Physics, Vienna*
[14]*Institute of High Energy Physics, Protvino*
[15]*INFN-Sezione di Torino, Torino*
[16]*Institute for Theoretical and Experimental Physics, Moscow*
[17]*J. Stefan Institute, Ljubljana*
[18]*Kanagawa University, Yokohama*
[19]*Institut für Experimentelle Kernphysik, Karlsruher Institut für Technologie, Karlsruhe*
[20]*Korea Institute of Science and Technology Information, Daejeon*
[21]*Korea University, Seoul*
[22]*Kyungpook National University, Taegu*
[23]*École Polytechnique Fédérale de Lausanne (EPFL), Lausanne*
[24]*Faculty of Mathematics and Physics, University of Ljubljana, Ljubljana*
[25]*Luther College, Decorah, Iowa 52101*
[26]*University of Maribor, Maribor*
[27]*Max-Planck-Institut für Physik, München*
[28]*University of Melbourne, School of Physics, Victoria 3010*
[29]*Graduate School of Science, Nagoya University, Nagoya*

[30]Kobayashi-Maskawa Institute, Nagoya University, Nagoya
[31]Nara Women's University, Nara
[32]National Central University, Chung-li
[33]National United University, Miao Li
[34]Department of Physics, National Taiwan University, Taipei
[35]H. Niewodniczanski Institute of Nuclear Physics, Krakow
[36]Nippon Dental University, Niigata
[37]Niigata University, Niigata
[38]University of Nova Gorica, Nova Gorica
[39]Osaka City University, Osaka
[40]Pacific Northwest National Laboratory, Richland, Washington 99352
[41]Research Center for Electron Photon Science, Tohoku University, Sendai
[42]University of Science and Technology of China, Hefei
[43]Seoul National University, Seoul
[44]Sungkyunkwan University, Suwon
[45]School of Physics, University of Sydney, NSW 2006
[46]Tata Institute of Fundamental Research, Mumbai
[47]Excellence Cluster Universe, Technische Universität München, Garching
[48]Tohoku Gakuin University, Tagajo
[49]Tohoku University, Sendai
[50]Department of Physics, University of Tokyo, Tokyo
[51]Tokyo Institute of Technology, Tokyo
[52]Tokyo Metropolitan University, Tokyo
[53]Tokyo University of Agriculture and Technology, Tokyo
[54]CNP, Virginia Polytechnic Institute and State University, Blacksburg, Virginia 24061
[55]Wayne State University, Detroit, Michigan 48202
[56]Yamagata University, Yamagata
[57]Yonsei University, Seoul

(Received 29 May 2012; published 6 December 2012)

We report the first evidence for the $\eta_b(2S)$ using the $h_b(2P) \to \eta_b(2S)\gamma$ transition and the first observation of the $h_b(1P) \to \eta_b(1S)\gamma$ and $h_b(2P) \to \eta_b(1S)\gamma$ transitions. The mass and width of the $\eta_b(1S)$ and $\eta_b(2S)$ are measured to be $m_{\eta_b(1S)} = (9402.4 \pm 1.5 \pm 1.8)$ MeV/c^2, $m_{\eta_b(2S)} = (9999.0 \pm 3.5^{+2.8}_{-1.9})$ MeV/c^2, and $\Gamma_{\eta_b(1S)} = (10.8^{+4.0+4.5}_{-3.7-2.0})$ MeV. We also update the $h_b(1P)$ and $h_b(2P)$ mass measurements. We use a 133.4 fb^{-1} data sample collected at energies near the $\Upsilon(5S)$ resonance with the Belle detector at the KEKB asymmetric-energy e^+e^- collider.

DOI: 10.1103/PhysRevLett.109.232002 PACS numbers: 14.40.Pq, 12.39.Pn, 13.25.Gv

Bottomonium, a bound system of a $b\bar{b}$ quark-antiquark pair, is well described by nonrelativistic quantum mechanics due to the slow motion of the heavy quarks [1]. The spin-singlet ($S = 0$) states of the quark pair with zero orbital momentum, $L = 0$, are customarily called $\eta_b(nS)$ with $n = 1, 2, \ldots$ The hyperfine splitting $\Delta M_{\rm HF}$ from the corresponding spin-triplet state, i.e., the mass difference between the $\Upsilon(nS)$ and $\eta_b(nS)$, provides an important measure of the spin-spin interaction between the quark and the antiquark. The existing measurements [2] of the $\eta_b(1S)$ mass are only in marginal agreement with theoretical expectations [3,4] and the $\eta_b(1S)$ width is yet to be measured. There is no information available on the radially excited state $\eta_b(2S)$.

In this Letter, we report the first evidence for the $\eta_b(2S)$ in the $h_b(2P) \to \eta_b(2S)\gamma$ transition and the first observation of the $h_b(1P) \to \eta_b(1S)\gamma$ and $h_b(2P) \to \eta_b(1S)\gamma$ transitions. We use a 121.4 fb^{-1} data sample at the $\Upsilon(5S)$ resonance and 12.0 fb^{-1} of energy-scan data collected nearby with the Belle detector [5] at the KEKB asymmetric-energy e^+e^- collider [6].

We study the processes $e^+e^- \to \Upsilon(5S) \to h_b(nP)\pi^+\pi^- \to [\eta_b(mS)\gamma]\pi^+\pi^-$ in which the $\eta_b(mS)$ states are reconstructed inclusively. The approximate values of the expected energies of the photons in the $h_b(nP)$ rest frame are given in Table I. The $h_b(nP)$ signal is tagged using the missing mass of the $\pi^+\pi^-$ pair $M_{\rm miss}(\pi^+\pi^-)$, while the $\eta_b(mS)$ signal is tagged using the variable

TABLE I. Expected photon energies in $h_b(nP) \to \eta_b(mS)\gamma$ transitions (E_γ), π^0 veto parameters (ΔM and $E_{\rm th}$) and the parameter σ of the $M^{(n)}_{\rm miss}(\pi^+\pi^-\gamma)$ resolution function.

	E_γ, MeV	ΔM, MeV/c^2	$E_{\rm th}$, MeV	σ, MeV/c^2
$h_b(2P) \to \eta_b(2S)\gamma$	260	10	125	8.6 ± 0.7
$h_b(1P) \to \eta_b(1S)\gamma$	500	13	75	13.6 ± 1.1
$h_b(2P) \to \eta_b(1S)\gamma$	860	17	75	19.8 ± 1.1

$M^{(n)}_{\rm miss}(\pi^+\pi^-\gamma) \equiv M_{\rm miss}(\pi^+\pi^-\gamma) - M_{\rm miss}(\pi^+\pi^-) + m_{h_b(nP)}$. The missing mass is defined via $M_{\rm miss}(X) = \sqrt{(E_{\rm c.m.} - E^*_X)^2 - p^{*2}_X}$, where $E_{\rm c.m.}$ is the center-of-mass (c.m.) energy and E^*_X and p^*_X are the energy and momentum of the system X measured in the c.m. frame. We fit the $M_{\rm miss}(\pi^+\pi^-)$ spectra for different $M^{(n)}_{\rm miss}(\pi^+\pi^-\gamma)$ bins to measure the $h_b(nP)$ yield. This procedure removes the background due to random $\pi^+\pi^-$ combinations. The $h_b(nP)$ yield peaks at $M^{(n)}_{\rm miss}(\pi^+\pi^-\gamma)$ values corresponding to the masses of the $\eta_b(mS)$ states from the $h_b(nP) \to \eta_b(mS)\gamma$ transitions.

The selection criteria for the $\pi^+\pi^-$ pairs are the same as those described in Ref. [7]. We use events that pass the Belle-standard hadronic event selection and consider all positively identified $\pi^+\pi^-$ pairs that originate from the vicinity of the interaction point. Belle previously observed that the decay $\Upsilon(5S) \to h_b(nP)\pi^+\pi^-$ proceeds via the intermediate resonances $Z_b(10610)$ and $Z_b(10650)$ [8]. We exploit this with the additional requirement $10.59\ {\rm GeV}/c^2 < M_{\rm miss}(\pi^\pm) < 10.67\ {\rm GeV}/c^2$, which suppresses the combinatorial background by a factor of 5 [1.6] for the $h_b(1P)$ [$h_b(2P)$] without any significant loss of the signal. Photon candidates are clusters in the electromagnetic calorimeter that are not associated with charged tracks. We apply a veto on $\pi^0 \to \gamma\gamma$ decays, rejecting a photon candidate if the invariant mass of it and any other photon in the event with energy above the threshold $E_{\rm th}$ is within ΔM of the π^0 mass. The parameters $E_{\rm th}$ and ΔM, listed in Table I, are chosen by maximizing the ratio $\frac{S}{\sqrt{B}}$, where S is the number of signal events in the Monte Carlo (MC) simulation and B is the number of background events estimated from a small fraction (0.1%) of the data. To suppress continuum $e^+e^- \to q\bar{q}$ ($q = u, d, s, c$) background, we use the ratio R_2 of the second- to zeroth-order Fox-Wolfram moments [9]. In the $\eta_b(1S)$ analysis, we require $R_2 < 0.3$, which was optimized using the $\Upsilon(5S) \to \Upsilon(2S)\pi^+\pi^-$ decays [7]. For the high statistics $h_b(1P) \to \eta_b(1S)\gamma$ transition, the optimum is shifted to $R_2 < 0.32$, which we adopt here for the $\eta_b(2S)$ analysis.

To calibrate the photon energy resolution function, we use three control channels: $D^{*0} \to \gamma D^0(\to K^-\pi^+)$, $\pi^0 \to \gamma\gamma$ and $\eta \to \gamma\gamma$. For the two-photon final states, we require that the energies of the photons in the laboratory frame be almost equal: $|E_1 - E_2|/(E_1 + E_2) < 0.05$. This reduces the resolution shape dependence to a single variable. The resolution shape is parameterized by a double-sided bifurcated Crystal Ball function [10] in which a bifurcated Gaussian is smoothly joined with power law tails on both sides. The signal is extracted using the $M(K^-\pi^+\gamma) - M(K^-\pi^+) + m_{D^0}$ distribution for the D^{*0} and $M(\gamma\gamma)$ for the π^0 and η. From comparisons of the peak positions and widths in data and MC simulation, we determine shifts in the photon energy $\Delta E/E$ and width correction factors f as a function of E. Various calibration channels give consistent results; an uncertainty is assigned based on their spread. These translate to typical mass shift and width-correction factors of $1.2\ {\rm MeV}/c^2$ and 1.13, respectively. Average values of left and right widths (σ) of the bifurcated Gaussian components of the $M^{(n)}_{\rm miss}(\pi^+\pi^-\gamma)$ resolution functions are given in Table I.

We update previous Belle measurements of the $h_b(nP)$ masses [7], incorporating a 10% increase in statistics and the requirement of an intermediate Z_b [11]. The results of the fits are shown in Figs. 1 and 2 and the fitted signal parameters are listed in Table II. The confidence level of the fit in the $h_b(1P)$ [$h_b(2P)$] region is 35% [70%]. The estimation of systematic uncertainties follows Ref. [7]. For hyperfine splittings $\sum_{J=0}^{2}\frac{2J+1}{9} m_{\chi_{bJ}(nP)} - m_{h_b(nP)}$, we find $\Delta M_{\rm HF}(1P) = (+0.8 \pm 1.1)\ {\rm MeV}/c^2$ and $\Delta M_{\rm HF}(2P) = (+0.5 \pm 1.2)\ {\rm MeV}/c^2$, where statistical and systematic uncertainties in mass are added in quadrature.

We fit the $M_{\rm miss}(\pi^+\pi^-)$ spectra for each $M^{(n)}_{\rm miss}(\pi^+\pi^-\gamma)$ bin to measure the $h_b(nP)$ yield as a function of $M^{(n)}_{\rm miss}(\pi^+\pi^-\gamma)$. We fix the masses of the peaking components at the values given in Table II. Although the $M_{\rm miss}(\pi^+\pi^-)$ combinatorial background shape in the $h_b(2P)$ region is rather complicated (described by an eighth-order Chebyshev polynomial), it changes slowly with $M^{(2)}_{\rm miss}(\pi^+\pi^-\gamma)$. For the $M_{\rm miss}(\pi^+\pi^-)$ fits for each bin, we multiply the polynomial shape with parameters fixed at their values from the overall fit by a lower-order polynomial with floating coefficients; this procedure improves the accuracy of the $h_b(nP)$ yield measurements.

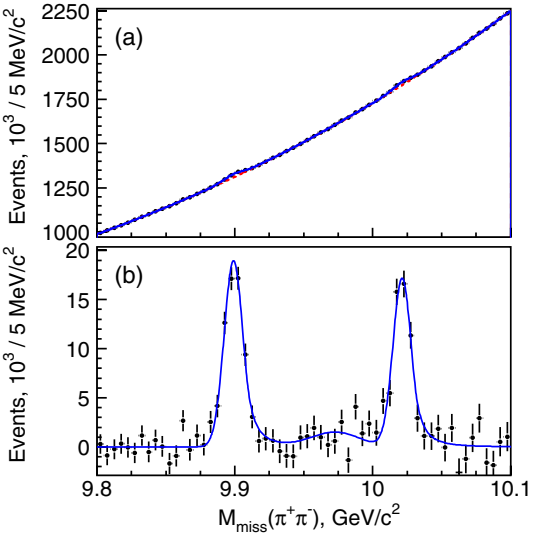

FIG. 1 (color online). The $M_{\rm miss}(\pi^+\pi^-)$ spectrum in the $h_b(1P)$ region. In (a) the data are the points with error bars with the fit function (blue solid curve) and background (red dashed curve) overlaid. (b) The background subtracted data (points with error bars) while the signal component of the fit is overlaid (blue curve). The background is combinatorial.

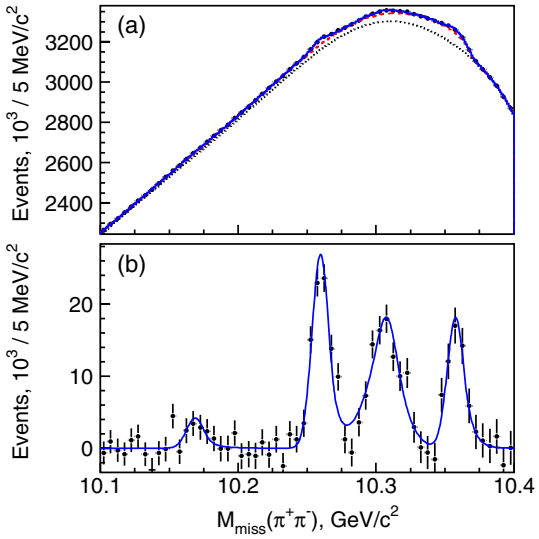

FIG. 2 (color online). The $M_{\rm miss}(\pi^+\pi^-)$ spectrum in the $h_b(2P)$ region. The legend is the same as in Fig. 1. The background components are random combinations and $K^0_S \to \pi^+\pi^-$ decays. The combinatorial component is shown in (a) by the black dotted curve.

For this lower-order function, we use a first- (fifth-) order polynomial for the $\eta_b(1S)$ [$\eta_b(2S)$] $M^{(2)}_{\rm miss}(\pi^+\pi^-\gamma)$ region. From a generic MC simulation, we find that the $K^0_S \to \pi^+\pi^-$ contribution is independent of the $M^{(2)}_{\rm miss}(\pi^+\pi^-\gamma)$ value in the $\eta_b(1S)$ region; in the $\eta_b(2S)$ region, we restrict the $M_{\rm miss}(\pi^+\pi^-)$ fit range to 10.10 GeV/c^2–10.34 GeV/c^2, thereby avoiding the sharp rise in the $K^0_S \to \pi^+\pi^-$ contribution that occurs at 10.37 GeV/c^2. The results for the $h_b(1P)$ and $h_b(2P)$ yields as a function of $M^{(n)}_{\rm miss}(\pi^+\pi^-\gamma)$ are presented in Fig. 3. Clear peaks at 9.4 GeV/c^2 and 10.0 GeV/c^2 are identified as signals for the $\eta_b(1S)$ and $\eta_b(2S)$, respectively. Generic MC simulations indicate that no peaking backgrounds are expected in these spectra.

We fit the $h_b(nP)$ yield dependence on $M^{(n)}_{\rm miss}(\pi^+\pi^-\gamma)$ to a sum of the $\eta_b(nS)$ signal components described by the convolution of a nonrelativistic Breit-Wigner function with the calibrated resolution function described above and a background parameterized by an exponentiation of a first- (second-) order polynomial in the $\eta_b(1S)$ [$\eta_b(2S)$] region. The two $M^{(n)}_{\rm miss}(\pi^+\pi^-\gamma)$ spectra [from the $h_b(1P)$ and $h_b(2P)$] with $\eta_b(1S)$ signals are fitted simultaneously. We take into account the effect of multiple photons in the same $M^{(n)}_{\rm miss}(\pi^+\pi^-\gamma)$ bin by increasing the errors in the corresponding $M_{\rm miss}(\pi^+\pi^-)$ histogram. We find event yields for the $h_b(nP) \to \eta_b(mS)$ transitions of $N_{1P\to1S} = (23.5 \pm 2.0) \times 10^3$, $N_{2P\to1S} = (10.3 \pm 1.3) \times 10^3$ and $N_{2P\to2S} = (25.8 \pm 4.9) \times 10^3$; the fitted masses and width are $m_{\eta_b(1S)} = (9402.4 \pm 1.5 \pm 1.8)$ MeV/c^2, $\Gamma_{\eta_b(1S)} = (10.8^{+4.0+4.5}_{-3.7-2.0})$ MeV and $m_{\eta_b(2S)} = (9999.0 \pm 3.5^{+2.8}_{-1.9})$ MeV/c^2. The confidence level of the $\eta_b(1S)$ [$\eta_b(2S)$] fit is 61% [36%]. If the $\eta_b(2S)$ width is allowed to float in the fit, we find $\Gamma_{\eta_b(2S)} = (4^{+12}_{-20})$ MeV or $\Gamma_{\eta_b(2S)} < 24$ MeV at 90% C.L. using the Feldman-Cousins approach [12]. For the $\eta_b(2S)$ mass determination

TABLE II. The yield and mass of peaking components from the fits to the $M_{\rm miss}(\pi^+\pi^-)$. Here and everywhere in this Letter, the first quoted uncertainty is statistical (unless stated otherwise) and the second (if present) is systematic.

	N, 10^3	Mass, MeV/c^2
$\Upsilon(5S) \to h_b(1P)$	$70.3 \pm 3.3^{+1.9}_{-0.7}$	$9899.1 \pm 0.4 \pm 1.0$
$\Upsilon(3S) \to \Upsilon(1S)$	13 ± 7	9973.0
$\Upsilon(5S) \to \Upsilon(2S)$	61.3 ± 4.1	10021.3 ± 0.5
$\Upsilon(5S) \to \Upsilon(1D)$	14 ± 7	10169 ± 3
$\Upsilon(5S) \to h_b(2P)$	$89.5 \pm 6.1^{+0.0}_{-5.8}$	$10259.8 \pm 0.5 \pm 1.1$
$\Upsilon(2S) \to \Upsilon(1S)$	97 ± 12	10305.6 ± 1.2
$\Upsilon(5S) \to \Upsilon(3S)$	58 ± 8	10357.7 ± 1.0

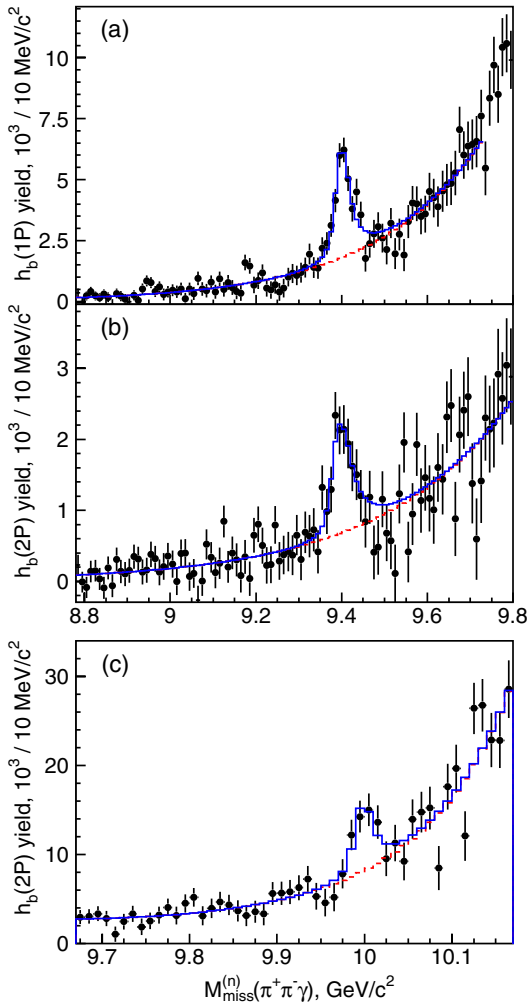

FIG. 3 (color online). The $h_b(1P)$ yield vs $M^{(1)}_{\rm miss}(\pi^+\pi^-\gamma)$ (a), and $h_b(2P)$ yield vs $M^{(2)}_{\rm miss}(\pi^+\pi^-\gamma)$ in the $\eta_b(1S)$ region (b) and in the $\eta_b(2S)$ region (c). The solid (dashed) histogram is the fit result (background component of the fit function).

and yield measurements quoted above, we fix the $\eta_b(2S)$ width at its value from perturbative calculations [13] $\Gamma_{\eta_b(2S)} = \Gamma_{\eta_b(1S)} \frac{\Gamma_{ee}^{\Upsilon(2S)}}{\Gamma_{ee}^{\Upsilon(1S)}} = (4.9^{+2.7}_{-1.9})$ MeV, where the uncertainty is due to our experimental uncertainty in $\Gamma_{\eta_b(1S)}$.

To estimate the systematic uncertainties in the $\eta_b(nS)$ parameters, we vary the polynomial orders and fit intervals in the $M_{\rm miss}(\pi^+\pi^-)$ & $M^{(n)}_{\rm miss}(\pi^+\pi^-\gamma)$ fits, and the $M^{(n)}_{\rm miss}(\pi^+\pi^-\gamma)$ binning by scanning the starting point of the 10 MeV/c^2 bin with 1 MeV/c^2 steps. We also multiply the nonrelativistic Breit-Wigner function by an E_γ^3 term expected for an electric dipole transition and include the uncertainty in the $h_b(1P)$ and $h_b(2P)$ masses and in the estimated value of the $\eta_b(2S)$ width. The contribution of each source is given in Table III. We add the various contributions in quadrature to estimate the total systematic uncertainty. We repeat the analysis using signal MC simulation instead of data and find no shift of the $\eta_b(nS)$ parameters compared to the MC input. For the hyperfine splittings $m_{\Upsilon(nS)} - m_{\eta_b(nS)}$ we determine $\Delta M_{\rm HF}(1S) = (57.9 \pm 2.3)$ MeV/c^2 and $\Delta M_{\rm HF}(2S) = (24.3^{+4.0}_{-4.5})$ MeV/c^2, where statistical and systematic uncertainties in mass are added in quadrature.

Using Wilks's theorem [14], we find 15σ [9σ] for the $h_b(1P) \to \eta_b(1S)\gamma$ [$h_b(2P) \to \eta_b(1S)\gamma$] statistical significance. For the significance of the $\eta_b(2S)$ signal, we use a method that takes into account the trial factor associated with the definition of the search window or the so-called "look-elsewhere effect" [15]. To determine this window, we conservatively assume $r = 0$ and $r = 1$ for the ratio $r = \frac{\Delta M_{\rm HF}(2S)}{\Delta M_{\rm HF}(1S)}$. (For reference, the measured value of $r = 0.420^{+0.071}_{-0.079}$ is consistent with perturbative calculations [16] that predict $\frac{m^2_{\Upsilon(2S)}}{m^2_{\Upsilon(1S)}} \frac{\Gamma_{ee}^{\Upsilon(2S)}}{\Gamma_{ee}^{\Upsilon(1S)}} = 0.513 \pm 0.011$, where the error is due to the uncertainties in Γ_{ee}.) We find the significance of the $\eta_b(2S)$ signal to be 4.8σ (4.2σ including systematics).

Branching fractions $\mathcal{B}[h_b(nP) \to \eta_b(mS)\gamma]$ are determined from $N^{\rm total}_{nP\to mS}/(N^{\rm total}_{nP}\epsilon)$, where $N^{\rm total}_{nP\to mS} = N_{nP\to mS} + N^{\text{anti-cut}}_{nP\to mS}$ and $N^{\rm total}_{nP} = N_{nP} + N^{\text{anti-cut}}_{nP}$, $N^{\text{anti-cut}}_{nP\to mS}$ [$N^{\text{anti-cut}}_{nP}$] is the number of the $h_b(nP) \to \eta_b(mS)\gamma$ transitions [$h_b(nP)$] that are rejected by the R_2 and π^0 veto requirements [by the R_2 requirement], ϵ is the reconstruction efficiency of the photon. In this way, we do not rely on MC simulation for the determination of the efficiency of the R_2 and π^0 veto requirements. To determine $N^{\text{anti-cut}}_{nP}$ and $N^{\text{anti-cut}}_{nP\to mS}$, we repeat the analysis for the events rejected by the corresponding requirements. In the $M^{(n)}_{\rm miss}(\pi^+\pi^-\gamma)$ [$M_{\rm miss}(\pi^+\pi^-)$] fits, we fix the $\eta_b(mS)$ mass and width [the $h_b(nP)$ mass]. We estimate the $N^{\text{anti-cut}}_{nP}$ systematic uncertainty by varying the polynomial order and fit range in the $M_{\rm miss}(\pi^+\pi^-)$ fit and by varying the $h_b(nP)$ mass within its uncertainty. We find $N^{\rm total}_{1P} = (84.2 \pm 4.4^{+2.1}_{-1.3}) \times 10^3$ and $N^{\rm total}_{2P} = (98.5 \pm 8.1^{+5.5}_{-6.3}) \times 10^3$. For $N^{\rm total}$, we add the N and $N^{\text{anti-cut}}$ uncertainties in quadrature. The contributions from the various sources of systematic uncertainty to the $N^{\rm total}_{nP\to mS}$ are given in Table IV. The $h_b(nP)$ signal shape uncertainty is not considered for the yields, since it cancels in the ratio $N^{\rm total}_{nP\to mS}/N^{\rm total}_{nP}$. In combining the $N_{nP\to mS}$ and $N^{\text{anti-cut}}_{nP\to mS}$ uncertainties, we take into account correlations of the calibration and $\eta_b(nS)$ line shape sources. We find $N^{\rm total}_{1P\to 1S} = (30.9 \pm 3.2^{+3.4}_{-1.8}) \times 10^3$, $N^{\rm total}_{2P\to 1S} = (16.1 \pm 2.4^{+2.0}_{-2.2}) \times 10^3$ and $N^{\rm total}_{2P\to 2S} = (35.6 \pm 7.3^{+4.5}_{-5.4}) \times 10^3$.

The efficiency is determined using phase-space MC simulated events that we weight according to the expectation $1 - \cos^2\theta_\gamma + 2\cos\theta_\gamma \cos\theta_{\pi^+} \cos\theta_{\pi^+\gamma}$ [17], where θ_γ (θ_{π^+}) is the angle between the beam axis and γ (π^+) momentum and $\theta_{\pi^+\gamma}$ is the angle between γ and π^+ momenta, with all momenta measured in the c.m. frame. Efficiencies to reconstruct the photon after the $\pi^+\pi^-$ pair is already reconstructed are 74.6% for $h_b(1P) \to \eta_b(1S)\gamma$, 73.4% for $h_b(2P) \to \eta_b(1S)\gamma$ and 76.1% for $h_b(2P) \to \eta_b(2S)\gamma$. The $\eta_b(1S)$ [$\eta_b(2S)$] signal function is normalized to unity in the mass window 9.3 GeV/c^2–9.5 GeV/c^2 [9.9 GeV/c^2–10.1 GeV/c^2]; thus, the yields and efficiencies correspond to this mass window. The efficiencies have relative uncertainties of 2% due to possible differences between the data and MC simulation, and $^{+0.7}_{-0.8}$% [$^{+0.5}_{-0.6}$%] due to the uncertainty in the $\eta_b(1S)$

TABLE III. Systematic uncertainties in the $\eta_b(1S)$ and $\eta_b(2S)$ masses (in MeV/c^2) and in the $\eta_b(1S)$ width (in MeV).

	$m_{\eta_b(1S)}$	$\Gamma_{\eta_b(1S)}$	$m_{\eta_b(2S)}$
$M_{\rm miss}(\pi^+\pi^-)$ fits	$^{+0.1}_{-0.2}$	$^{+0.0}_{-0.8}$	$^{+0.0}_{-0.1}$
$M^{(n)}_{\rm miss}(\pi^+\pi^-\gamma)$ binning	$^{+0.2}_{-0.5}$	$^{+0.7}_{-0.8}$	$^{+2.3}_{-1.4}$
$M^{(n)}_{\rm miss}(\pi^+\pi^-\gamma)$ fit	$^{+0.2}_{-0.0}$	$^{+4.2}_{-0.6}$	$^{+0.5}_{-0.2}$
Calibration	± 1.4	± 1.5	± 0.7
$\eta_b(nS)$ line shape	$^{+0.6}_{-0.0}$	$^{+0.0}_{-0.4}$	$^{+0.6}_{-0.0}$
$h_b(nP)$ mass	± 0.9	± 0.0	± 1.1
$\eta_b(2S)$ width	-	-	$^{+0.1}_{-0.0}$
Total	± 1.8	$^{+4.5}_{-2.0}$	$^{+2.8}_{-1.9}$

TABLE IV. Systematic uncertainties in the total yields of the $h_b(1P) \to \eta_b(1S)\gamma$, $h_b(2P) \to \eta_b(1S)\gamma$ and $h_b(2P) \to \eta_b(2S)\gamma$ transitions (in 10^3).

	$N^{\rm total}_{1P\to 1S}$	$N^{\rm total}_{2P\to 1S}$	$N^{\rm total}_{2P\to 2S}$
$M_{\rm miss}(\pi^+\pi^-)$ fits	$^{+0.2}_{-1.1}$	$^{+1.6}_{-1.8}$	$^{+0.0}_{-1.3}$
$M^{(n)}_{\rm miss}(\pi^+\pi^-\gamma)$ binning	$^{+1.0}_{-0.3}$	$^{+0.5}_{-0.1}$	$^{+1.5}_{-3.7}$
$M^{(n)}_{\rm miss}(\pi^+\pi^-\gamma)$ fit	$^{+3.2}_{-1.2}$	$^{+1.0}_{-1.3}$	$^{+2.5}_{-2.1}$
Calibration	$^{+0.3}_{-0.4}$	± 0.0	± 1.3
$\eta_b(nS)$ line shape	$^{+0.2}_{-0.0}$	$^{+0.1}_{-0.0}$	$^{+0.3}_{-0.0}$
$\eta_b(nS)$ mass & width	$^{+0.7}_{-0.5}$	± 0.3	$^{+3.1}_{-2.8}$
Total	$^{+3.4}_{-1.8}$	$^{+2.0}_{-2.2}$	$^{+4.5}_{-5.4}$

$[\eta_b(2S)]$ width. We find $\mathcal{B}[h_b(1P) \to \eta_b(1S)\gamma] = (49.2 \pm 5.7^{+5.6}_{-3.3})\%$, $\mathcal{B}[h_b(2P) \to \eta_b(1S)\gamma] = (22.3 \pm 3.8^{+3.1}_{-3.3})\%$ and $\mathcal{B}[h_b(2P) \to \eta_b(2S)\gamma] = (47.5 \pm 10.5^{+6.8}_{-7.7})\%$. These branching fractions are a factor of 1.2 to 2.5 higher than theoretical expectations [18].

In summary, we report the first evidence for the $\eta_b(2S)$ using the $h_b(2P) \to \eta_b(2S)\gamma$ transition, with a significance, including systematics, of 4.2σ, and the first observation of the $h_b(1P) \to \eta_b(1S)\gamma$ and $h_b(2P) \to \eta_b(1S)\gamma$ transitions. The mass and width parameters of the $\eta_b(1S)$ and $\eta_b(2S)$ are measured to be $m_{\eta_b(1S)} = (9402.4 \pm 1.5 \pm 1.8)\ \mathrm{MeV}/c^2$, $m_{\eta_b(2S)} = (9999.0 \pm 3.5^{+2.8}_{-1.9})\ \mathrm{MeV}/c^2$ and $\Gamma_{\eta_b(1S)} = (10.8^{+4.0+4.5}_{-3.7-2.0})$ MeV. The $m_{\eta_b(2S)}$ and $\Gamma_{\eta_b(1S)}$ are first measurements; the $m_{\eta_b(1S)}$ measurement is more precise than the current world average and is $(11.4 \pm 3.6)\ \mathrm{MeV}/c^2$ above the central value [19]. The hyperfine splittings, $\Delta M_{\mathrm{HF}}(1S) = (57.9 \pm 2.3)\ \mathrm{MeV}/c^2$, $\Delta M_{\mathrm{HF}}(2S) = (24.3^{+4.0}_{-4.5})\ \mathrm{MeV}/c^2$ and their ratio $0.420^{+0.071}_{-0.079}$, are in agreement with theoretical calculations [4,20]. We update the $h_b(1P)$ and $h_b(2P)$ mass measurements $m_{h_b(1P)} = (9899.1 \pm 0.4 \pm 1.0)\ \mathrm{MeV}/c^2$, $m_{h_b(2P)} = (10259.8 \pm 0.5 \pm 1.1)\ \mathrm{MeV}/c^2$, and $1P$ and $2P$ hyperfine splittings $\Delta M_{\mathrm{HF}}(1P) = (+0.8 \pm 1.1)\ \mathrm{MeV}/c^2$, $\Delta M_{\mathrm{HF}}(2P) = (+0.5 \pm 1.2)\ \mathrm{MeV}/c^2$. These results supersede those in Ref. [7].

We are grateful to A. M. Badalian, Yu. S. Kalashnikova, and M. B. Voloshin for useful discussions. We thank the KEKB group for excellent operation of the accelerator; the KEK cryogenics group for efficient solenoid operations; and the KEK computer group, the NII, and PNNL/EMSL for valuable computing and SINET4 network support. We acknowledge support from MEXT, JSPS and Nagoya's TLPRC (Japan); ARC and DIISR (Australia); NSFC (China); MSMT (Czechia); DST (India); INFN (Italy); MEST, NRF, GSDC of KISTI, and WCU (Korea); MNiSW (Poland); MES and RFAAE (Russia); ARRS (Slovenia); SNSF (Switzerland); NSC and MOE (Taiwan); and DOE and NSF (USA).

[1] N. Brambilla *et al.*, Eur. Phys. J. C **71**, 1534 (2011).
[2] B. Aubert *et al.* (*BABAR* Collaboration), Phys. Rev. Lett. **101**, 071801 (2008); B. Aubert *et al.* (*BABAR* Collaboration), Phys. Rev. Lett. **103**, 161801 (2009); G. Bonvicini *et al.* (CLEO Collaboration), Phys. Rev. D **81**, 031104 (2010).
[3] B. A. Kniehl, A. A. Penin, A. Pineda, V. A. Smirnov, and M. Steinhauser, Phys. Rev. Lett. **92**, 242001 (2004); **104**, 199901(E) (2010).
[4] See, for example, S. Meinel, Phys. Rev. D **82**, 114502 (2010).
[5] A. Abashian *et al.* (Belle Collaboration), Nucl. Instrum. Methods Phys. Res., Sect. A **479**, 117 (2002).
[6] S. Kurokawa and E. Kikutani, Nucl. Instrum. Methods Phys. Res., Sect. A **499**, 1 (2003), and other papers included in this volume.
[7] I. Adachi *et al.* (Belle Collaboration), Phys. Rev. Lett. **108**, 032001 (2012).
[8] A. Bondar *et al.* (Belle Collaboration), Phys. Rev. Lett. **108**, 122001 (2012).
[9] G. C. Fox and S. Wolfram, Phys. Rev. Lett. **41**, 1581 (1978).
[10] J. E. Gaiser, Ph.D. thesis, SLAC-R-255, 1982 (unpublished); T. Skwarnicki, Ph.D. thesis, DESY F31-86-02, 1986 (unpublished).
[11] Comparing to Ref. [7], the Z_b requirement changed the shape of the combinatorial background. Therefore, the polynomial order was modified to obtain the highest C.L. The $h_b(1P)$ and $h_b(2P)$ regions are described, respectively, by a 3rd order and 8th order Chebyshev polynomial instead of a 5th and 7th order. In addition, the fit interval is reduced by decreasing the end point from 10.45 to 10.40 GeV/c^2.
[12] G. J. Feldman and R. D. Cousins, Phys. Rev. D **57**, 3873 (1998).
[13] W. Kwong, P. Mackenzie, R. Rosenfeld, and J. Rosner, Phys. Rev. D **37**, 3210 (1988) (and references therein); R. Barbieri, G. Curci, E. d' Emilio, and E. Remiddi, Nucl. Phys. **B154**, 535 (1979).
[14] S. S. Wilks, Ann. Math. Stat. **9**, 60 (1938).
[15] E. Gross and O. Vittels, Eur. Phys. J. C **70**, 525 (2010).
[16] R. Van Royen and V. F. Weisskopf, Nuovo Cimento A **50**, 617 (1967); **51**, 583 (1967); T. Appelquist, R. M. Barnett, and K. D. Lane, Annu. Rev. Nucl. Part. Sci. **28**, 387 (1978).
[17] M. Voloshin (private communications).
[18] S. Godfrey and J. L. Rosner, Phys. Rev. D **66**, 014012 (2002).
[19] J. Beringer *et al.* (Particle Data Group), Phys. Rev. D **86**, 010001 (2012).
[20] R. J. Dowdall *et al.* (HPQCD Collaboration), Phys. Rev. D **85**, 054509 (2012). The ratio $\Delta M_{\mathrm{HF}}(2S)/\Delta M_{\mathrm{HF}}(1S)$ calculated in this paper is in agreement with our measurement, while the individual values of the hyperfine splittings are higher than our results.